

Estimation of fusion time in heavy-ion collisions

B. Sahu* and C. S. Shastry

Department of Physics, North-Eastern Hill University, Shillong 793003, India

(Received 7 April 1988)

The time for fusion process is estimated by evaluating the time spent by the classical Coulomb trajectory and Coulomb-nuclear trajectory within the fusion formation region $r < R_F$. The parameter R_F is taken from the recent works of Udagawa *et al.* Our estimate of fusion time extends the results of Scalia to a larger number of pairs of nuclei and energies. We find that the fusion time above the barrier obtained by using classical Coulomb-nuclear trajectories which is of the order of 10^{-22} to 10^{-21} s is about five times larger than the times obtained using Coulomb trajectories. We also see that fusion times for different partial waves are of the same order and do not vary much with angular momentum. We further adopt the quantum-mechanical phase-shift method used by Munzinger and Berkowitz to estimate the fusion time both below and above the barrier. In agreement with their general conclusion, we find that fusion time is oscillatory above the barrier and decreases rapidly with decrease in energy below the barrier up to certain energy. However, at still lower energy it starts increasing rapidly. The order of magnitude of oscillatory time above the barrier falls in between the times obtained using classical Coulomb trajectories and Coulomb-nuclear trajectories. But the trend in the sub-barrier region is physically not well understood. We take an alternative approach to estimate the fusion formation time below the barrier by assuming fusion to be a reverse decay process caused by the incident flux of projectiles on the target. This calculation of fusion time is done within the framework of the WKB method. We find that fusion formation time just below the barrier is of the order of 10^{-23} s and starts increasing very rapidly with decrease in energy. In this case, we find that fusion formation time is larger than the corresponding time for free transit across the barrier. On the other hand, in the phase-shift method fusion time is found to be smaller than the free time in some cases. It is observed that fusion time, in general, is larger for identical nuclei than that for nonidentical pairs of nuclei.

I. INTRODUCTION

An important aspect of heavy-ion fusion reactions is the time scale involved in fusion process. There have been a number of works estimating the time scale from different viewpoints. Munzinger and Berkowitz¹ obtained this time scale by estimating the time delay within the framework of a barrier penetration model. Bonasera² compared a time-dependent-Hartree-Fock (TDHF) based classical model with the experimental data and estimated the interaction time. Bertsch³ has obtained the fusion time by calculating the time to reach local equilibrium considering the equilibration of deformed Fermi sphere within the Fermi-gas approximation. Scalia⁴ calculates the fusion time by estimating the time spent by the system within the interaction region using classical Rutherford trajectory.

In this paper we present the results obtained for fusion time for a variety of systems and energies both below and above the Coulomb barrier. First we consider the following simple picture of fusion to estimate fusion time. Recent works⁵⁻⁷ have described the fusion process by separating the heavy-ion interaction into two separate rate regions: (i) $r < R_F = r_F(A_T^{1/3} + A_P^{1/3})$ within which fusion process is assumed to take place, and (ii) $r > R_F$ which describes peripheral processes. Therefore, it is desirable that the fusion time is estimated by calculating the time spent by the heavy-ion system in region $r < R_F$.

Adopting the approach of Scalia⁴ one may evaluate the interaction time spent by the system along the Coulomb trajectory within $r < R_F$. A more realistic way to do this is to evaluate the time spent by the system in the region $r < R_F$ using Coulomb-nuclear (CN) trajectory corresponding to both the Coulomb and nuclear potentials. In this connection it is to be noted that such a calculation should be carried out for a number of partial waves to get a meaningful picture of fusion time. Because, *a priori*, it is not clear whether time spent within the region $r < R_F$ by the system in different angular momentum (l) states varies rapidly with l or not, even for partial waves which are lower than the orbiting partial waves. The classical estimation of time for an orbiting partial wave will be infinitely large if the corresponding effective barrier is located within the region $r < R_F$. In this paper we present, in a systematic manner, the fusion time for a variety of nucleus-nucleus systems evaluated by using both Coulomb trajectories and CN trajectories for a number of partial waves and energies in order to get a comprehensive idea of fusion time.

The classical approach discussed above is not adequate for estimating the fusion time below the effective barrier for any particular partial wave. In such cases the approach of Munzinger and Berkowitz¹ is of interest. In their approach, they evaluated the time delay⁸⁻¹⁰ corresponding to tunneling through the relevant interaction barrier. One of the puzzling aspects of their results,

which is observed by them, is the gradual decrease of the fusion time as the center-of-mass energy (E) decreases such that the difference ($V_B - E$) between the barrier top (V_B) and E increases. In this paper we consider this problem again and bring out some more aspects of their model at very low energies.

In view of the puzzling aspects of the results in Ref. 1, we consider an alternative picture of the fusion below the barrier in order to estimate the fusion time. We treat fusion as a sort of "inverse" of decay in which the system approaches the barrier and tunnels through it and gets fused. The probability of penetration through the barrier will naturally depend on the incident flux and the interaction region available to the incident flux to undergo fusion. Just as in the simple alpha decay mode where one evaluates the decay constant (λ) and mean life (λ^{-1}), we evaluate the "fusion formation constant" (λ_F) by considering it as a tunneling problem from outside the barrier to inside and then estimate the fusion time (λ_F^{-1}) within such model. It is interesting to note that orders of magnitude of time obtained by this method and that from the method of Munzinger and Berkowitz¹ are same in the vicinity of the barrier but have entirely different behavior at lower energies.

Section II discusses the fusion time obtained using classical Coulomb trajectory and Coulomb-nuclear trajectory. In Sec. III, we deal with the evaluation of time using the phase-shift method within the framework of barrier penetration model. Section IV considers the fusion formation constant and the corresponding lifetime using the framework of barrier penetration model and the WBK approximation. Section V deals with the discussions and conclusion.

II. FUSION TIME ABOVE BARRIER FROM CLASSICAL TRAJECTORY

Recently there have been several works⁵⁻⁷ which describe the fusion process by assuming an interaction parameter r_F such that fusion reaction is confined to $r < R_F$, where $R_F = r_F(A_T^{1/3} + A_P^{1/3})$ and A_T , A_P denote the mass numbers of target and projectile, respectively. On the other hand, the earlier approach to fusion (the sharp cutoff model) assumed that the fusion is confined to the orbital angular momentum $l < l_{cr}$, where l_{cr} is close to the grazing angular momentum. In evaluating the fusion

time using classical Coulomb or Coulomb-nuclear trajectories, we incorporate both these aspects.

The time spent by a classical trajectory within $r < R_F$ can be formally expressed as

$$T = 2 \int_{R_{\min}}^{R_F} \frac{dr}{\dot{r}}. \quad (1)$$

Here R_{\min} is the distance of closest approach where radial kinetic energy vanishes. In the case of Coulomb trajectory the expression for time (T_C) is

$$T_C = (2\mu)^{1/2} \int_{R_{\min}}^{R_F} \frac{dr}{[E - V_C(r) - V_l(r)]^{1/2}}. \quad (2)$$

Here E denotes the center-of-mass energy, V_C is the Coulomb potential, V_l is the centrifugal term, and μ is the reduced mass.

We assume $V_C(r)$ of the form

$$V_C(r) = \frac{Z_T Z_P e^2}{2R_C} (3 - r^2/R_C^2), \quad r \leq R_C$$

$$= \frac{Z_T Z_P e^2}{r}, \quad r \geq R_C,$$

where

$$R_C = r_C (A_T^{1/3} + A_P^{1/3})$$

and

$$V_l(r) = \frac{\hbar^2 l(l+1)}{2\mu r^2}.$$

The symbols Z_T , Z_P denote the proton number of the target and the projectile, respectively, and r_C denotes the Coulomb radius parameter.

We get from Eq. (2)

$$T_C = (2\mu)^{1/2} \left[\int_{R_{\min}}^{R_C} \frac{dr}{[E - V_C(r) - V_l(r)]^{1/2}} + \int_{R_C}^{R_F} \frac{dr}{[E - V_C(r) - V_l(r)]^{1/2}} \right]. \quad (3)$$

Equation (3) can be evaluated analytically to get the Coulomb trajectory time T_C in 10^{-23} s as

TABLE I. Optical potential parameters (Ref. 6) and the corresponding barrier height V_B and its position R_B for $l=0$.

Systems	V_0 (MeV)	r_0 (fm)	a_R (fm)	r_C (fm)	r_F (fm)	V_B (MeV)	R_B (fm)
$^{16}\text{O} + ^{208}\text{Pb}$	100.0	1.25	0.50	1.25	1.45	73.84	12.25
$^{16}\text{O} + ^{148}\text{Sm}$	20.0	1.34	0.57	1.25	1.46	59.46	11.25
$^{40}\text{Ar} + ^{122}\text{Sn}$	41.8	1.25	0.51	1.25	1.50	107.83	11.39
$^{40}\text{Ca} + ^{40}\text{Ca}$	35.0	1.35	0.43	1.35	1.46	53.19	10.25
$^{58}\text{Ni} + ^{58}\text{Ni}$	40.0	1.25	0.55	1.25	1.45	100.22	10.56
$^{58}\text{Ni} + ^{64}\text{Ni}$	40.0	1.25	0.55	1.25	1.45	98.61	10.75
$^{58}\text{Ni} + ^{124}\text{Sn}$	58.1	1.26	0.294	1.26	1.42	165.10	11.88
$^{64}\text{Ni} + ^{118}\text{Sn}$	58.1	1.26	0.294	1.26	1.46	164.22	11.95
$^{81}\text{Br} + ^{90}\text{Zr}$	35.0	1.35	0.43	1.35	1.41	154.45	12.49

$$T_C \approx 10.18 \left[2 \frac{A_T A_P}{A_T + A_P} \right]^{1/2} \left[\frac{1}{2(a')^{1/2}} \ln[2a'x + b' + 2(a'^2 x^2 + a'b'x + a'C')^{1/2}] \right]_{x=X_{\min}}^{x=X_C} \\ + 10.18 \left[2 \frac{A_T A_P}{A_T + A_P} \right]^{1/2} \left[\frac{(ax^2 + bx + c)^{1/2}}{a} - \frac{b}{2a^{3/2}} \ln[2ax + b + 2(a^2 x^2 + abx + ac)^{1/2}] \right]_{x=R_C}^{x=R_F},$$

where

$$a' = 1.4398 Z_T Z_P / 2R_C^3, \\ b' = [E - 3(1.4398 Z_T Z_P / 2R_C)], \\ c' = -41.815(l^2 + l) / 2[A_T A_P / (A_T + A_P)], \\ a = E, \\ b = -1.4398 Z_T Z_P, \\ c = -41.815(l^2 + l) / 2[A_T A_P / (A_T + A_P)], \\ X_{\min} = (R_{\min})^2,$$

and

$$X_C = (R_C)^2.$$

We evaluate T_C for different systems and energies choosing different values of l up to $l = l_G$, where l_G is the grazing partial wave. The approximate expression for l_G is

$$l_G = [kR_B(kR_B - 2\eta)]^{1/2},$$

where

$$R_B = \frac{Z_T Z_P e^2}{V_B}, \\ k^2 = \frac{2\mu E}{\hbar^2},$$

and

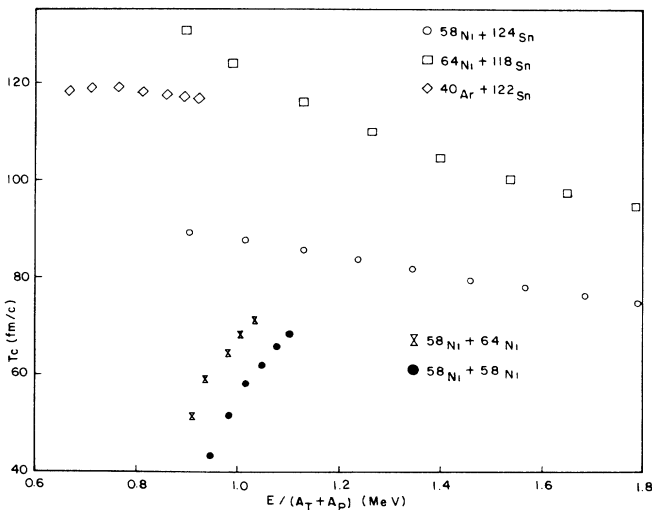


FIG. 1. Fusion time T_C obtained using classical Coulomb trajectory with $l = l_G$ for five pairs of nuclei at different energies.

$$\eta = \frac{Z_T Z_P e^2 \mu}{\hbar^2 k}.$$

V_B , R_B , and η denote s -wave barrier height, radius of the barrier peak, and Rutherford parameter, respectively.

When the real part of nuclear potential is added to $V_C(r)$ and $V_l(r)$, the corresponding expression for time (T_{CN}) spent within the region $R'_{\min} < r < R_F$ is given by

$$T_{CN} = (2\mu)^{1/2} \int_{R'_{\min}}^{R_F} \frac{dr}{[E - V_n(r) - V_C(r) - V_l(r)]^{1/2}}, \quad (4)$$

where $V_n(r)$ denotes the nuclear potential which is assumed to be having the usual Woods-Saxon forms with parameters V_0 , r_0 , and a_R . R'_{\min} in this case will be different from R_{\min} which occurs when only Coulomb potential is considered. In Table I we summarize the various nucleus-nucleus systems and potential parameters taken from Ref. 6 and used in our calculations.

In Fig. 1 we show the variation of the Coulomb trajectory time T_C elapsed within the region $r < R_F$ as a function of $E / (A_T + A_P)$ for orbital angular momentum $l = l_G$. The time is of the order of 10^{-22} s. The results shown in Fig. 1 supplement the fusion time data given in Ref. 4 for several pairs of interacting nuclei not considered there. These confirm the fact that times involved are of the order of 10^{-22} s if classical Coulomb trajectories are used to evaluate the fusion time for $l = l_G$. In Fig. 2, we show the values of fusion time T_{CN} obtained

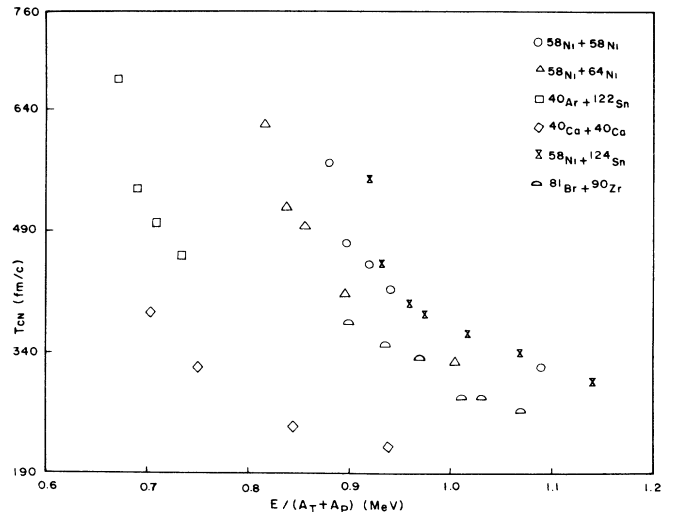


FIG. 2. Fusion time T_{CN} obtained using classical Coulomb-nuclear trajectory with $l = l_G - 5$ for six pairs of nuclei at different energies.

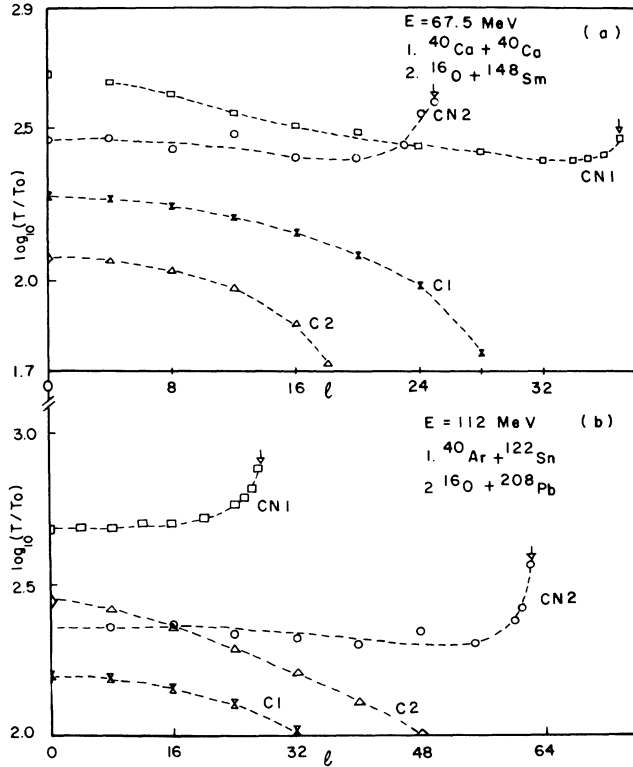


FIG. 3. (a) Variation $\log_{10}(T/T_0)$ corresponding to $T=T_C$ and $T=T_{CN}$ with l for classical Coulomb (C) and Coulomb-nuclear (CN) trajectories, respectively, for $^{40}\text{Ca}+^{40}\text{Ca}$ and $^{16}\text{O}+^{148}\text{Sm}$ at center-of-mass energy $E=67.5$ MeV. $T_0=1$ fm/c $=0.333 \times 10^{-23}$ s. Arrow indicates grazing partial wave ($l=l_G$) where orbiting mechanism occurs. (b) Same as (a) for systems $^{40}\text{Ar}+^{122}\text{Sn}$ and $^{16}\text{O}+^{208}\text{Pb}$ at $E=112$ MeV.

using the Coulomb-nuclear trajectory for various systems and for a particular $l < l_G$. Comparison of Figs. 1 and 2 shows that effect of the attractive nuclear potential increases the time spent by the system within $r < R_F$ by a factor of about 5. One finds that fusion time from a Coulomb-nuclear trajectory is of the order of 10^{-21} s.

In the above calculation we have used a particular partial wave to evaluate the fusion time. It is of interest to see the variation of the fusion time with orbital angular momentum l . In this connection it is necessary to note that if only Coulomb potential is taken, the effective potential $V_C(r)+V_l(r)$ does not have any potential pocket or a barrier. On the other hand, the effective potential $V_n(r)+V_C(r)+V_l(r)$ shows a barrier and a pocket for a number of partial waves, which can cause classical orbiting at particular energies. In Figs. 3(a) and 3(b), we show the variation of fusion times T_C and T_{CN} with l . In the case of Coulomb trajectories, one notices that the variation of T_C with l is, in general, quite small for l up to l_G . Hence, representing the typical order of fusion time as that corresponding to trajectory having $l=l_G$ is reasonable. Figures 3(a) and 3(b) also show the variation of

fusion time T_{CN} with l corresponding to CN trajectories. In this case it is also seen that for $l < l_G$, the fusion time has practically the same order of magnitude for different values of l . However, as l approaches l_G the time increases rapidly due to the onset of orbiting phenomena. This is a rather special case and occurs due to the purely classical model. In actuality, due to quantum effects and the imaginary part of the potential, the barrier top states corresponding to orbiting have finite lifetime. In view of these observations, we have used, for the calculation of typical fusion time T_{CN} , the partial wave $l < l_G$. In conclusion, we find that the fusion times calculated for a number of systems using classical Coulomb trajectories are in the range 1×10^{-22} s to 5×10^{-22} s, whereas times calculated using CN trajectories are in the range 6×10^{-22} s to 2×10^{-21} s. One also observe the following aspects from Fig. 3(a) and 3(b): (i) In Fig. 3(b), the difference $T_{CN}-T_C$ is seen to be larger for $^{40}\text{Ar}+^{122}\text{Sn}$ than the corresponding difference for the $^{16}\text{O}+^{208}\text{Pb}$ system. The main difference between these two, as far as Fig. 3(b) is concerned, is that in the case of the $^{40}\text{Ar}+^{122}\text{Sn}$ system $E-V_B \approx 5$ MeV, whereas in the case of the $^{16}\text{O}+^{208}\text{Pb}$ system $E-V_B \approx 39$ MeV. (ii) Figure 3(a) shows that the fusion time for an identical pair of nuclei is larger than the time for a nonidentical pair of nuclei. All of these calculations and the conclusion pertain to the cases when the energy is above the effective barrier. In the next two sections we estimate the fusion time below the effective barrier using semiclassical methods.

III. FUSION TIME BELOW THE BARRIER BY PHASE-SHIFT METHOD

In order to estimate the fusion time below the barrier we now consider the approach to Munzinger and Berkowitz¹ within the framework of barrier penetration model. The method is briefly outlined as follows.⁸⁻¹⁰ Let us consider a rectangular potential barrier of approximately chosen width a and height V_0 , i.e.,

$$\begin{aligned} V(x) &= 0, & x < 0 \\ &= V_0, & 0 \leq x \leq a \\ &= 0, & x > a \end{aligned} \quad (5)$$

Considering the case $E < V_0$, E being the total energy of the incident particle of mass m , the solutions of the Schrödinger equation in three regions can be written as

$$\begin{aligned} &= Ae^{ikx} + Be^{-ikx}, & x < 0 \\ &= Ce^{k_1x} + De^{-k_1x}, & 0 \leq x \leq a \\ &= Fe^{ikx}, & x > a \end{aligned} \quad (6)$$

where $k = (2mE/\hbar^2)^{1/2}$, and $k_1 = [2m(V_0-E)/\hbar^2]^{1/2}$. Using the proper continuity conditions at the boundaries we get¹¹

$$F/A = \frac{(-i)4kk_1 e^{-ika} e^{k_1 a}}{(k - ik_1)^2 - (k + ik_1)^2 e^{2k_1 a}}, \quad (7)$$

which leads to the expression for transmission coefficient $T = |F/A|^2$. The phase shift⁹ obtained from the argu-

$$\frac{d\alpha(k)}{dk} = \left[\frac{1}{k_1} \right] \left[\frac{(2mV_0/\hbar^2)^2 \sinh(2k_1 a) - 2ak^2 k_1 (k^2 - k_1^2)}{4k^2 k_1^2 \cosh^2 k_1 a + (k^2 - k_1^2)^2 \sinh^2 k_1 a} \right] - a. \quad (9)$$

The transmission time^{1,9} (\mathcal{T}_{PS}) corresponding to the penetration of barrier of width a is

$$\mathcal{T}_{PS} = \frac{m}{k\hbar} \left[\frac{d\alpha(k)}{dk} + a \right]. \quad (10)$$

Further we may write

$$k_1 a = \beta(1 - \epsilon)^{1/2},$$

where

$$\beta = [2mV_0 a^2 / \hbar^2]^{1/2},$$

and

$$\epsilon = E/V_0.$$

When $k_1 a \gg 1$, using Eqs. (9) and (10) we get an approximation expression for \mathcal{T}_{PS} in the form

$$\mathcal{T}_{PS} = \frac{\hbar}{V_0 [\epsilon(1 - \epsilon)]^{1/2}} \times [1 - 4\beta\epsilon(2\epsilon - 1)(1 - \epsilon)^{1/2} e^{-2\beta(1 - \epsilon)^{1/2}}]. \quad (11)$$

The condition $k_1 a \gg 1$ is valid for typical heavy-ion systems and energies. For the case $E > V_0$, the analysis is very similar, except that, in the region $0 \leq x \leq a$, instead of the solutions $e^{\pm k_1 x}$ we will have solution $e^{\pm ik_2 x}$ where $k_2 = [2m(E - V_0)/\hbar^2]^{1/2}$.

Taking this into account we get the phase shift⁹ of transmitted wave in the form

$$\gamma(k) = \tan^{-1} \left[\frac{(k^2 + k_2^2) \tan(ak_2)}{2kk_2} \right] - ak, \quad (12)$$

and the expression for time \mathcal{T}_{PS} above the barrier is

$$\begin{aligned} \mathcal{T}_{PS} &= \frac{m}{\hbar k} \left[\frac{d\gamma(k)}{dk} + a \right] \\ &= \frac{m}{\hbar k k_2} \frac{2ak^2 k_2 (k^2 + k_2^2) - (2mV_0/\hbar^2)^2 \sin(2ak_2)}{4k^2 k_2^2 \cos^2(ak_2) + (k^2 + k_2^2)^2 \sin^2(ak_2)}. \end{aligned} \quad (13)$$

The calculation in Ref. 1 using the above approach shows that the fusion time is of the order of 10^{-22} s. As a function of E , it has a sharp peak corresponding to the barrier top, decreases in an oscillatory way above the barrier, decreases rapidly without any oscillation below the barrier up to certain energy and then rate of decrease becomes

ment of (F/A) is

$$\alpha(k) = \tan^{-1} \left[\frac{k^2 - k_1^2}{2kk_1} \tanh k_1 a \right] - ka, \quad (8)$$

which gives

quite small with further decrease in energy. The time \mathcal{T}_{PS} above the barrier obtained from Eq. (13) is shown in Fig. 4. Here V_0 corresponds to the barrier height $V_B (\approx 165 \text{ MeV})$ for $l=0$ for the system $^{58}\text{Ni} + ^{124}\text{Sn}$ and the width of the barrier (a) is taken approximately as 6 fm. The time \mathcal{T}_{PS} decreases in an oscillatory way. The oscillations are quite rapid near the barrier. It is also seen that these oscillations are more rapid than the case studied in Ref. 1 which corresponds to a light heavy-ion system. \mathcal{T}_{PS} is found to lie, however, in between the times T_C and T_{CN} obtained from classical trajectories. As noted in Ref. 1, smaller values of fusion time below the barrier as compared to the above barrier case is somewhat puzzling. We expect that as the difference $(V_B - E)$ increases, fusion time should also increase indicating decrease in probability of fusion. In order to explain this point further, we explore \mathcal{T}_{PS} in the energy region close to zero. From our expression (11) it is clear that the variation of time \mathcal{T}_{PS} should show a rapid increase as E approaches zero. This is shown in Fig. 5. It is clear that

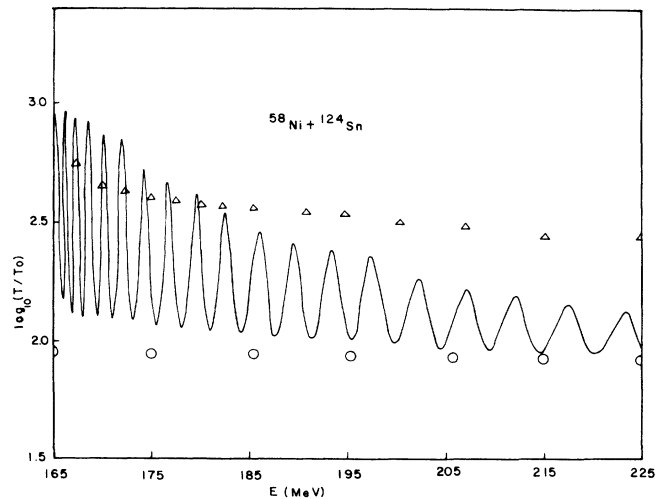


FIG. 4. Oscillatory variation of $\log_{10}(T/T_0)$ corresponds to fusion time $T = \mathcal{T}_{PS}$ above barrier obtained using the phase-shift method. Open circles and triangles denote $\log_{10}(T_C/T_0)$ for $l=l_G$ and $\log_{10}(T_{CN}/T_0)$ for $l=l_G - 5$, respectively, corresponding to $^{58}\text{Ni} + ^{124}\text{Sn}$. The height of the rectangular barrier used to calculate \mathcal{T}_{PS} corresponds to the s -wave height of the Coulomb barrier of the same system (i.e., $V_0 = V_B = 165 \text{ MeV}$). The width of the barrier taken is 6 fm.

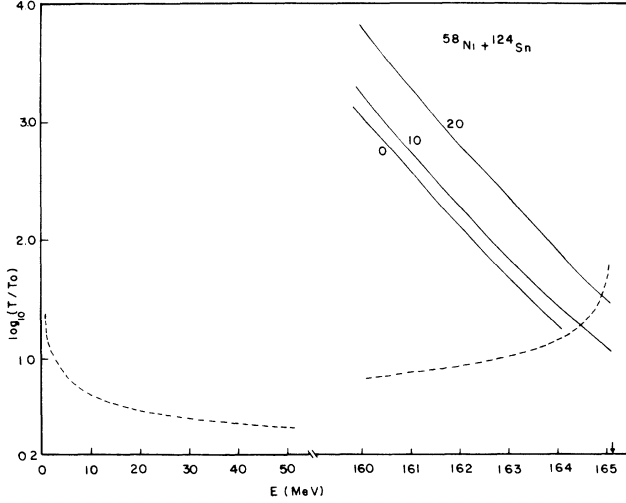


FIG. 5. Variation (dashed line) of $\log_{10}(T/T_0)$ corresponding to $T = T_{PS}$ obtained by the phase-shift method below the barrier in the case of rectangular barrier specified in Fig. 4. The solid line shows the variation $\log_{10}(T/T_0)$ corresponding to $T = T_F$ obtained using the fusion formation time method. The numbers in the figure indicate the angular momentum quantum number l . The arrow indicates the barrier height.

T_{PS} decreases rapidly with decrease in energy when one goes down the barrier until $(\epsilon = E/V_0) \simeq 0.5$ and starts gradually increasing again with further decrease in energy. This shows that fusion time estimated by the above approach is quite sensitive to energy and significance of this pattern is not clear. In view of this, in the next section we give a somewhat different approach for estimation of fusion time within the barrier penetration model. This gives a rapid increase of fusion time with decrease in energy below the barrier.

IV. FUSION FORMATION TIME BELOW THE BARRIER

The problem of fusion of two interacting nuclei can be treated as due to absorption of the incident wave corresponding to the equivalent one-body problem after it tunnels through the barrier. Hence, the problem is to calculate the "fusion formation constant" (λ_F) akin to the cal-

ulation of decay constant in the barrier penetration model of alpha decay. The inverse of the formation constant λ_F can be taken to represent the fusion formation time (T_F) below the barrier. One recalls that in the calculation of decay constant in alpha decay, one has to incorporate the frequency of collision of the alpha particle with the potential barrier. The analogous situation here is the frequency with which the two nuclei come together to fuse in the interaction region as a result of the incidence of flux of projectile nuclei over the target nuclei.

Let us consider that at the center-of-mass energy E the effective potential has turning points r_3 , r_2 , and r_1 , such that $r_3 > r_2 > r_1$ and $r_3 - r_2$ specifies the barrier region. Within semiclassical picture, r_3 denotes the radius of the interaction region, the penetration into which by the two nuclei can cause fusion. With this physical picture we can write the fusion formation constant λ_F as

$$\lambda_F = T_r F_r, \quad (14)$$

where T_r denotes the transmission coefficient and F_r is the frequency with which the two nuclei come to a distance $R = r_3$, which is the outermost turning point, to fuse. Using the WKB approximation¹¹ the transmission coefficient T_r can be expressed as

$$T_r = \frac{1}{(1/\theta + \theta/4)^2}, \quad (15)$$

with

$$\theta = \exp \left[- \int_{r_2}^{r_3} \{ 2\mu [V(r) - E] / \hbar^2 \}^{1/2} dr \right].$$

Here

$$V(r) = V_n(r) + V_C(r) + V_l(r).$$

$V_n(r)$, $V_C(r)$, and $V_l(r)$ denote nuclear, Coulomb, and centrifugal terms of the effective potential $V(r)$, respectively. In the case of incident normalized plane wave, frequency F_r can be expressed as

$$F_r = C^2 \pi R^2 v, \quad (16)$$

where

$$C = (2\pi)^{-3/2} (\text{fm})^{-3/2}$$

and

TABLE II. Fusion formation time T_F and free transit time T_{fr} at sub-barrier energies.

Systems	V_B (MeV)	E (MeV)	a (fm)	T_F (fm/c)	T_{fr} (fm/c)
$^{40}\text{Ca} + ^{40}\text{Ca}$	53.19	49.69	1.95	1854	26
		50.44	1.7	557	23
		51.94	1.1	60	15
		52.69	0.7	24	9
$^{58}\text{Ni} + ^{124}\text{Sn}$	165.1	155.1	1.7	3×10^5	18
		162.1	0.85	121	9
		163.1	0.70	44	7
		164.1	0.45	18	5

TABLE III. Phase-shift time \mathcal{T}_{PS} and free transit time \mathcal{T}_{fr} at sub-barrier energies with reference to the system $^{58}\text{Ni} + ^{124}\text{Sn}$ where $V_B = 165$ MeV.

E (MeV)	$a=1$ fm		$a=2$ fm		$a=6$ fm	
	\mathcal{T}_{PS} (fm/c)	\mathcal{T}_{fr} (fm/c)	\mathcal{T}_{PS} (fm/c)	\mathcal{T}_{fr} (fm/c)	\mathcal{T}_{PS} (fm/c)	\mathcal{T}_{fr} (fm/c)
161.0	7.43	10.70	7.69	21.40	7.69	64.20
162.0	8.29	10.67	8.81	21.34	8.82	64.02
163.0	9.47	10.63	10.64	21.26	10.69	63.78
164.0	11.17	10.60	14.28	21.20	14.72	63.60
164.5	12.32	10.59	18.02	21.18	19.9	63.55
165.0	13.79	10.57	25.67	21.14	46.42	63.42

$$v = \frac{\hbar k}{\mu}.$$

Then the time of fusion formation (\mathcal{T}_F) is taken as

$$\mathcal{T}_F = \frac{1}{\lambda_F}. \quad (17)$$

In Fig. 5 we show \mathcal{T}_F as a function of energy for the system $^{58}\text{Ni} + ^{124}\text{Sn}$ for typical partial waves. It is clear that \mathcal{T}_F increases very rapidly with decrease in energy as one goes below the barrier. This is consistent with the fact that fusion formation probability should decrease with decrease in energy. However, it is interesting to note that the formation time just below the barrier is $\geq 10^{-23}$ s. On the other hand, we have seen that time spent by the interacting systems within the interaction region $r < R_F$ above the barrier, calculated using classical trajectories, is of the order of 10^{-22} to 10^{-21} s. Thus the time just below the barrier peak is found to be smaller than the time above the barrier. This particular aspect may be related to the enhancement of fusion below the barrier. For comparison purpose, in Fig. 5, we depict the results obtained by the phase-shift method below the barrier expressed by Eq. (11). It is seen that \mathcal{T}_{PS} decreases until $E/V_B \approx 0.5$ and then it starts increasing with further decrease of energy. It is clear from the expression (11) that it would be infinitely large at energy near zero and also at the barrier top energy V_B . On the other hand, the formation time \mathcal{T}_F is finite near the barrier and then increases exponentially with decrease in energy as seen from the approximate linear dependence of $\log_{10}(\mathcal{T}_F/T_0)$ with E .

For a particle of mass μ and speed v the time required to traverse a distance a is given by

$$\mathcal{T}_{fr} = \frac{a}{v}. \quad (18)$$

Let us call this time in the field free region as the free transit time \mathcal{T}_{fr} . Considering a to be the width of the barrier at certain sub-barrier energy E , we estimate the time \mathcal{T}_{fr} in the field free region. This time \mathcal{T}_{fr} is compared with the corresponding time \mathcal{T}_F which is the fusion formation time in the presence of the potential barrier. These times \mathcal{T}_F and \mathcal{T}_{fr} are listed in Table II. It is seen that \mathcal{T}_F is always greater than the corresponding \mathcal{T}_{fr} . On the other hand, in Ref. 1 it is stated that in the sub-barrier region \mathcal{T}_{PS} is less than the corresponding \mathcal{T}_{fr} . This is physically difficult to comprehend because it im-

plies that it is easier (takes less time) to penetrate a barrier than transmit the same distance when barrier is absent. Therefore, we consider this point in some detail to see whether the result $\mathcal{T}_{PS} < \mathcal{T}_{fr}$ is generally true within the framework of phase-shift method. In Table III, we list \mathcal{T}_{PS} and \mathcal{T}_{fr} for several barriers of different widths at different energies. It is seen from this table that near the barrier and for small a ($=1$ fm), $\mathcal{T}_{PS} > \mathcal{T}_{fr}$. Hence, in general, the statement $\mathcal{T}_{PS} < \mathcal{T}_{fr}$ is not correct. However, as stated earlier, \mathcal{T}_F is found to be greater than the corresponding \mathcal{T}_{fr} in all the cases that we have considered.

In Fig. 6, we show the variations of \mathcal{T}_F as a function of $(V_B - E)$ for systems of identical nuclei $^{40}\text{Ca} + ^{40}\text{Ca}$ and $^{58}\text{Ni} + ^{58}\text{Ni}$, and compare them with \mathcal{T}_F obtained in the

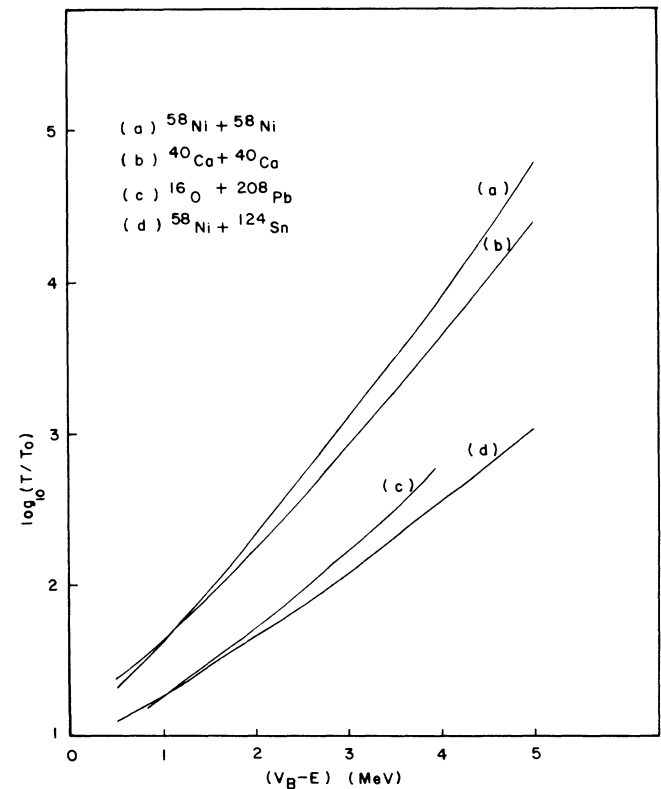


FIG. 6. Variation of $\log_{10}(T/T_0)$ with $(V_B - E)$ corresponding to $T = \mathcal{T}_F$ for two pairs of identical nuclei and two pairs of nonidentical nuclei.

case of pairs of nonidentical nuclei $^{16}\text{O} + ^{208}\text{Pb}$ and $^{58}\text{Ni} + ^{124}\text{Sn}$. As in the case of \mathcal{T}_{CN} and \mathcal{T}_{C} above barrier [see Fig. 3(a)], we find that \mathcal{T}_{F} corresponding to identical nuclei is larger than that in the case of nonidentical pairs of nuclei.

V. DISCUSSION AND CONCLUSION

In this paper we have estimated the fusion time for a number of nucleus-nucleus systems above the barrier by assuming that fusion reaction takes place within interaction region $r < R_{\text{F}}$. For the calculation of the fusion time above the barrier, we have used classical Coulomb trajectories and Coulomb-nuclear trajectories. It is found that if one uses CN trajectory, estimated fusion time ($\sim 6 \times 10^{-22}$ to 2×10^{-21} s) is larger than the corresponding time ($\sim 5 \times 10^{-22}$ s) calculated using Coulomb trajectory. In general, variation of fusion time obtained for different fusing partial waves is small. The calculation of \mathcal{T}_{CN} using classical Coulomb-nuclear trajectories gives infinitely large value when one approaches the orbiting partial wave as it should. However, considering the fact that effective potential has imaginary part and the system is essentially quantum mechanical, classical time corresponding to orbital partial wave is not physical. The fusion times obtained in this paper using Coulomb trajectories supplement those given in Ref. 4. Following the phase-shift method used in Ref. 1, we have estimated the time above the barrier within the framework of barrier penetration model and this is found to decrease in an oscillatory way with energy, giving rapid oscillations near the top of the effective barrier. From the result of Ref. 1

and our result it is clear that the oscillations critically depend on the barrier parameters and energy. The fusion times from classical trajectories, however, are found to be of same order of magnitude as that found in this approach above the barrier.

Coming to the energy region below the effective barrier, the time estimated by the same-phase shift method is large near the barrier and goes on decreasing when one goes down the barrier. However, the time again increases with the energy approaching zero. Thus the time is minimum at certain energy in between zero and the top of the barrier. The relevance of this behavior of time with energy is not clear so far as the fusion process is concerned. On the other hand, as an alternative procedure, we estimate the fusion formation time in sub-barrier region by considering fusion as a reversal decay process. In this approach we have shown that the fusion formation time (10^{-23} s) is small near the barrier and keeps on increasing exponentially with the decrease of energy from the top of the barrier. This sort of variation of fusion time with sub-barrier energy is quite consistent with the process of fusion below the threshold: fusion is more probable near the barrier and decreases with the decrease in energy. However, the orders of magnitude of times from this approach and the phase-shift method are same near the barrier. We also find that fusion time, in general, for a nonidentical pair of nuclei is smaller than that for two identical nuclei. It is also found that fusion time obtained by the phase-shift method is not always smaller than the time for the free transit of the same region. On the other hand, \mathcal{T}_{F} obtained using fusion formation time approach is found to be larger than the corresponding free time in all the cases considered by us.

*On leave from Physics Department, Gangadhar Meher College, Sambalpur 768004, Orissa, India.

¹P. Braun-Munzinger and G. M. Berkowitz, Phys. Lett. **125B**, 19 (1983).

²A. Bonasera, Lett. Nuovo Cimento **44**, 172 (1985).

³G. Bertsch, Z. Phys. A **289**, 103 (1978).

⁴A. Scalia, Nuovo Cimento A **92**, 210 (1986).

⁵T. Udagawa and T. Tamura, Phys. Rev. C **29**, 1922 (1984).

⁶T. Udagawa, B. T. Kim, and T. Tamura, Phys. Rev. C **32**, 124 (1985).

⁷T. Udagawa, S. W. Hong, and T. Tamura, Phys. Rev. C **32**, 1435 (1985).

⁸L. A. MacColl, Phys. Rev. **40**, 621 (1932).

⁹T. E. Hartman, J. Appl. Phys. **33**, 3427 (1962).

¹⁰E. P. Wigner, Phys. Rev. **98**, 145 (1955).

¹¹See, for example, A. K. Ghatak and S. Lokanathan, *Quantum Mechanics*, 3rd ed. (Macmillan India Limited, New Delhi, 1984), pp. 111 and 317; E. Merzbacher, *Quantum Mechanics*, 2nd ed. (Wiley, New York, 1970), p. 126.